INTERNATIONAL JOURNAL OF NUMERICAL METHODS IN FLUIDS, VOL. 13, 643–653 (1991)

MULTIDOMAIN COLLOCATION TECHNIQUES FOR A VISCOUS COMPRESSIBLE FLOW

BO KJELLMERT

Division of Physics, Luleå University of Technology, S-95187 Luleå, Sweden

SUMMARY

This paper presents a viscous compressible flow problem to which an equilibrium solution, in terms of density and velocity, can be given implicitly by elementary functions. The corresponding initial boundary value problem is solved by time discretization by the Crank–Nicolson method, Newton linearization and space discretization using multidomain Chebyshev collocation techniques. The physical interval is covered by subintervals of equal length. Each subinterval utilizes the same number of collocation points and each interface consists of one or two points. Six ways of patching are tested. All of them yield solutions with spectral accuracy for a few time steps, but only three are stable in the long run. Details of the density evolution are illustrated.

KEY WORDS Spectral multidomain method Patching methods Viscous compressible flow Shock structure

INTRODUCTION

The Burgers equation is a non-linear partial differential equation for which analytic solutions are known in terms of the initial conditions. It is a popular test problem for spectral schemes.[1] Among others, multidomain techniques have been applied to this problem.[2]

In this paper a similar but slightly more complicated test problem is presented for multidomain Chebyshev collocation schemes. We start from the compressible Navier–Stokes equations and, after some assumptions, arrive at an essentially parabolic system for the density and the velocity. An exact equilibrium solution to this problem can be constructed implicitly and can be matched to describe the structure of a steady shock.[3] The corresponding time-dependent one-dimensional system of equations is a suitable testbench for patching techniques.

The solution is advanced in time by the Crank–Nicolson method, the equations are linearized by a Newton method and then discretized in space. For simplicity the x-interval is composed of elements of equal length where each element utilizes the same number of collocation points. Six patching schemes are studied. Three of them are long-time stable. They involve

(i) explicit enforcement of continuity of functions and first derivatives across the interface
(ii) overlap—explicit enforcement of continuity of functions and first derivatives and collocation of governing differential equations across the interface
(iii) overlap—explicit enforcement of continuity of functions twice and collocation of governing differential equations across the interface.

0271–2091/91/150643–11$05.50
© 1991 by John Wiley & Sons, Ltd.

Received November 1989
Revised November 1990

BASIC EQUATIONS

The one-dimensional flow of a viscous compressible diatomic gas is described by

continuity equation

$$\partial\rho/\partial t + \rho\partial u/\partial x + u\partial\rho/\partial x = 0, \quad t\in]0, T], \quad x\in]-1, 1], \tag{1a}$$

momentum equation

$$\partial u/\partial t + (u/\gamma)\partial u/\partial x + (\theta/\gamma M^2\rho)\partial\rho/\partial x + [(\gamma-1)AM^2u/2\rho\sqrt{\theta}]\partial u/\partial x - [A\sqrt{(\theta)}/\rho]\partial^2 u/\partial x^2 = 0, \tag{1b}$$

where

$$\theta = 1-(\gamma-1)M^2u^2/2, \quad t\in]0, T], \quad x\in]-1, 1[,$$

boundary conditions

$$\rho = 1 \quad \text{and} \quad u = u_{\text{in}}, \quad x = -1,$$
$$u = u_{\text{out}}, \quad x = +1, \tag{1c}$$

initial conditions to be defined below.

In (1a–c) all quantities are non-dimensional; ρ is the mass density, u is the velocity, θ is the temperature, M is a Mach number, A is a dynamic viscosity and $\gamma = 1{\cdot}4$.

When deriving (1a–c), the dynamic viscosity has been assumed to be proportional to the square root of the temperature,[4] the pressure to be proportional to the density and the temperature, and the total enthalpy to be constant.

Equation (1a) is a hyperbolic equation for ρ and (1b) is a parabolic equation for u. The boundary conditions (1c) are therefore natural for positive u_{in} and u_{out}.

Equations (1a–c) represent a bad model of a real gas. There is, however, at least one exception. For air the total enthalpy remains constant throughout a steady shock.[3] Now u stands for the gas velocity relative to a frame attached to the shock, and the time-independent solution to (1a–c) gives the structure of a steady shock for appropriate values of the parameters. The steady solution is constructed implicitly by elementary functions; see Reference 5 for details. Now let

$$A = 0{\cdot}2, \qquad M = \sqrt{3}, \qquad u_{\text{in}} = 1, \qquad u_{\text{out}} = 0{\cdot}234\,243\,53. \tag{1d}$$

Then the equilibrium density and velocity profiles are obtained as shown in Figure 1. Obviously, only a section of the shock is studied—a section which contains more than half of the steep portion and is truncated where ρ and u reach almost constant values. This analytic solution, called AES, will provide suitable initial values of ρ and u when testing methods for solving the time-dependent equations (1).

Another smooth initial solution, (CFS) to (1a–c) is given by

$$u(x) = x(u_{\text{out}} - u_{\text{in}}) + (u_{\text{out}} + u_{\text{in}}),$$
$$\rho(x) = 1/u(x), \quad x\in[-1, 1].$$

Here u varies linearly between the boundaries, the parameters are given by (1d) and the flux ρu is constant. In the sequel the analytic equilibrium solution AES or the constant-flux solution CFS will define the initial conditions.

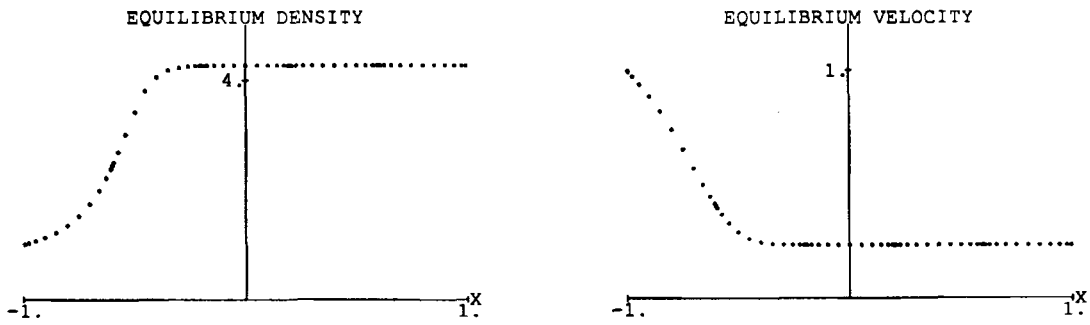

Figure 1. Density and velocity profiles for a steady shock (AES)

NUMERICAL PROCEDURE

Time discretization and linearization

The partial differential equations (1a, b) are time discretized by the Crank–Nicolson method. They then turn into ordinary differential equations for ρ $(=\rho^n)$ and u $(=u^n)$ at time $n\Delta t$, $n = 1, 2, \ldots$; the superscript denotes the time level and Δt is the time step. Initially, the density ρ^0 and the velocity u^0 are prescribed. Equations (1a–c) take the form

$$F_1(\rho, \partial\rho/\partial x, u, \partial u/\partial x) = 0, \quad x \in]-1, 1], \tag{2a}$$

$$F_2(\rho, \partial\rho/\partial x, u, \partial u/\partial x, \partial^2 u/\partial x^2) = 0, \quad x \in]-1, 1[, \tag{2b}$$

$$\rho = 1 \quad \text{and} \quad u = u_{\text{in}}, \quad x = -1,$$
$$u = u_{\text{out}}, \quad x = +1. \tag{2c}$$

The solution ρ, u to 2(a–c) is determined iteratively by a Newton method. Let the iteration number be denoted by the subscript k and let

$$\rho_0 = \rho^{n-1} \quad \text{and} \quad u_0 = u^{n-1}, \quad n = 1, 2, \ldots.$$

One anticipates that ρ_k, u_k converge towards ρ^n, u^n as k increases. To avoid cancellation, delta functions are introduced:

$$\Delta\rho_k = \rho_k - \rho^{n-1} \quad \text{and} \quad \Delta u_k = u_k - u^{n-1}, \quad k = 1, 2, \ldots.$$

For brevity the notation

$$\rho = \Delta\rho_k, \qquad u = \Delta u_k$$

will be used in the sequel until otherwise stated.

Expanding F_1 and F_2 in Taylor series around values evaluated at the previous iteration, (2a–c) become, after some algebra,

continuity equation

$$A_1\rho + B_1 u + C_1 \partial\rho/\partial x + D_1 \partial u/\partial x = H_1, \quad x \in]-1, 1], \tag{3a}$$

momentum equation

$$A_2\rho + B_2 u + C_2 \partial\rho/\partial x + D_2 \partial u/\partial x + \partial^2 u/\partial x^2 = H_2, \quad x \in]-1, 1[, \tag{3b}$$

boundary conditions

$$\rho = u = 0, \quad x = -1,$$
$$u = 0, \quad x = +1. \tag{3c}$$

The expressions for the coefficients $A_1, \ldots, H_2$ depend on functions evaluated at iteration number $k-1$. H_1 and H_2 also depend on functions from the previous time step $n-1$. Observe that F_1 and F_2 are not expanded around ρ^{n-1}, u^{n-1} but around ρ_{k-1}, u_{k-1}. The resulting coefficients therefore demand a new calculation for each iteration.

One-domain space discretization

By a standard Chebyshev collocation method a function $f(x)$, $x \in [-1, 1]$, is represented by the series

$$\sum_{j=0}^{N} a_j T_j(x),$$

where N is an integer and $T_j(x) = \cos(j \cos^{-1} x)$. The collocation points are $x_k = \cos(\pi k/N)$, $k = 0, 1, \ldots, N$ and the expansion coefficients are given by

$$a_j = (2/Nc_j) \sum_{k=0}^{N} (1/c_k) T_j(x_k) f_k, \quad j = 1, 2, \ldots, N,$$

with $f_k = f(x_k)$, $c_0 = c_N = 2$ and $c_j = 1$ for $j = 2, 3, \ldots, N-1$. The series representation approximates $f(x)$ for $x \in [-1, 1]$ and equals $f(x)$ at the collocation points.

The first and second derivatives of $f(x)$ are approximated by expansions with coefficients defined by the a_j. Differentiation matrices $\mathbf{D}^{(1)}$ and $\mathbf{D}^{(2)}$ are introduced such that

$$f'_k = \sum_{j=0}^{N} D^{(1)}_{kj} f_j \quad \text{and} \quad f''_k = \sum_{j=0}^{N} D^{(2)}_{kj} f_j, \quad k = 0, 1, \ldots, N.$$

The elements of $\mathbf{D}^{(1)}$ and $\mathbf{D}^{(2)}$ are well known.[6]

This formalism is applied to the functions $\rho(x)$ and $u(x)$ which satisfy (3). The equations can then be written in matrix form:

continuity equation

$$\sum_{j=0}^{N} (AM_{ij}\rho_j + BM_{ij}u_j) = H1_i, \tag{4a}$$

momentum equation

$$\sum_{j=0}^{N} (CM_{ij}\rho_j + DM_{ij}u_j) = H2_i, \tag{4b}$$

boundary conditions

$$\rho_N = 0, \qquad u_N = 0, \qquad u_0 = 0. \tag{4c}$$

By retaining all but the last ($i = N$) scalar equations in (4a) and all but the first ($i = 0$) and last scalar equations in (4b), and adding (4c), one derives a tractable matrix equation for the unknown

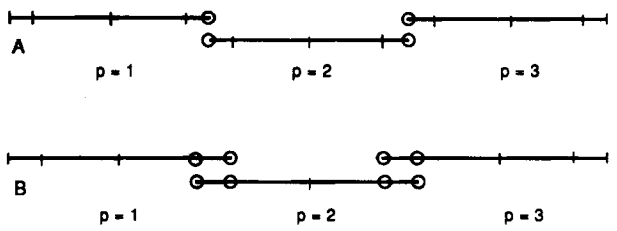

Figure 2. Nodes for $Q = 3$ and $N = 4$. Coinciding points are denoted by circles. The subintervals are labelled by the symbol p

vector

$$(\rho_1, \ldots, \rho_N, u_1, \ldots, u_N, \rho_0, \rho_N, u_0, u_N)^T.$$

In the multidomain context this method is called MUCHE with $Q = 1$, which is explained in the following subsection.

Multidomain discretization

The physical x-domain $[-1, 1]$ is covered by subintervals of equal length. Each subinterval is mapped onto a computational ξ-interval $[-1, 1]$, where standard Chebyshev collocation points are defined. By mapping back one obtains the corresponding nodes in the x-domain.

Let the number of subintervals be Q and the number of nodes in each subinterval be $N + 1$. Now two possible divisions exist. In fact, two adjacent subintervals may have one (A) or two (B) points in common (see Figure 2).

To be specific, the expressions for the nodes $x_{j,p}$ are given. Let the subinterval length be λ and introduce $\xi_j = \cos(\pi j/N)$. Then, for $j = 0, 1, \ldots, N$ and $p = 1, 2, \ldots, Q$,

$$\text{A:} \quad x_{j,p} = (\lambda/2)(\xi_j + 2p - 1) - 1, \quad \text{with } \lambda = 2/Q,$$

$$\text{B:} \quad x_{j,p} = (\lambda/2)\{\xi_j + p[1 + \cos(\pi/N)] - \cos(\pi/N)\} - 1, \quad \text{with}$$

$$\lambda = 4/\{(1 - \cos(\pi/N) + Q[1 + \cos(\pi/N)]\}.$$

The relation $\partial/\partial x = (2/\lambda)\partial/\partial\xi$ must be taken into account when differentiating. Then the one-domain matrix technique for transforming (3a, b) is easily extended to the multidomain case. Equations of the same form as (4a, b) are obtained for each subinterval. Hereafter (4a, b) also mean the fully discretized and linearized continuity and momentum equation respectively for a subinterval.

Here $x_{j,p}$ and $x_{i,q}$ are looked upon as different nodes if $j, p \neq i, q$, even when the two points coincide in physical space. By definition the interior points $x_{j,p}$ are labelled by (A) $j = 1, 2, \ldots N-2, N-1$, and (B) $j = 2, 3, \ldots, N-3, N-2$ for all p. Of course the exterior points $x_{j,p}$ are labelled by (A) $j = 0, N$ and (B) $j = 0, 1, N-1, N$ for all p. Let S be the union of all exterior points; S is an extended separator set. These definitions have been chosen because they give matrix equation (5) a simple structure.

In case A

$$S = \{x_{N,1}, x_{0,1}, x_{N,2}, \ldots, x_{0,Q-1}, x_{N,Q}, x_{0,Q}\}$$

and the conditions coupled with S are

inflow: $\rho = 0, u = 0$
interfaces: $\rho, u, \partial\rho/\partial x, \partial u/\partial x$ are continuous
outflow: $u = 0$, equation (4a) is satisfied.

In addition, (4a, b) are enforced at all interior points. To sum up, the collocated equations and the patching conditions yield $2Q(N-1)+2+4(Q-1)+2 = 2Q(N+1)$ scalar algebraic equations. It is clear that the total number of scalar algebraic equations equals the number of unknowns. The resulting procedure is called MUCHE. Alternatively, let ρ and u be continuous and (4a, b) be collocated at the interfaces. The corresponding procedure is called LUCHE. The patching conditions are explained further in Figure 3(a).

In case B the extended separator set is

$$S = \{x_{N,1}, x_{N-1,1}, x_{1,1}, x_{0,1}, \ldots, x_{N,Q}, x_{N-1,Q}, x_{1,Q}, x_{0,Q}\}.$$

Some of these points coincide in physical space:

$$x_{1,2} = x_{N,1}, x_{0,2} = x_{N-1,1}, \ldots, x_{1,Q} = x_{N,Q-1}, x_{0,Q} = x_{N-1,Q-1}.$$

The conditions satisfied at the inflow and outflow points are the same as those in case A while (4a, b) are collocated at the points nearest to the inflow and the outflow. At the subinterval interfaces the quantities ρ and u are continuous. The additional patching conditions may be specified in various ways. Here four options are considered; the corresponding procedures are called AICHE, BICHE, CICHE and DICHE; see Figure 3(b) for details. At the interior nodes equations (4a, b) are collocated. In all, the number of scalar equations is $2(N-3)Q+4+8(Q-1)+4 = 2(N+1)Q$.

Obviously, the six procedures differ in two ways. Firstly, the subintervals are patched in different ways. The procedures AICHE, BICHE, CICHE and MUCHE represent couplings of almost the same strength, while the coupling is stronger in DICHE and weaker in LUCHE. Secondly, MUCHE and LUCHE use one set of nodes and AICHE, BICHE, CICHE and DICHE another set. These sets are close to each other when the number of nodes in each subinterval is large.

All procedures are implemented analogously using the Schur complement method developed for elliptic partial differential equations.[7] Thus the scalar equations are permuted into the form

$$\begin{pmatrix} \mathbf{A}T_1 & & & & \mathbf{B}T_1 \\ & \mathbf{A}T_2 & & & \mathbf{B}T_2 \\ & & \ddots & & \vdots \\ & & & \mathbf{A}T_Q & \mathbf{B}T_Q \\ \mathbf{C}T_1 & \mathbf{C}T_2 & \cdots & \mathbf{C}T_Q & \mathbf{A}S \end{pmatrix} \begin{pmatrix} \mathbf{U}V_1 \\ \mathbf{U}V_2 \\ \vdots \\ \mathbf{U}V_Q \\ \mathbf{U}S \end{pmatrix} = \begin{pmatrix} \mathbf{R}V_1 \\ \mathbf{R}V_2 \\ \vdots \\ \mathbf{R}V_Q \\ \mathbf{R}S \end{pmatrix}, \tag{5}$$

where the unknown vectors are $\mathbf{U}V_p$, $p = 1, \ldots, Q$, and $\mathbf{U}S$. $\mathbf{U}V_p$ is built by the interior unknowns and $\mathbf{U}S$ by the exterior unknowns, i.e. by set S. The matrices $\mathbf{A}T_p$ and $\mathbf{B}T_p$ correspond to the continuity and momentum equations, while $\mathbf{C}T_1, \ldots, \mathbf{C}T_Q$ and $\mathbf{A}S$ correspond to the patching conditions.

In order to solve (5), one first eliminates $\mathbf{U}V_p$, $p = 1, \ldots, Q$, and gets an equation for $\mathbf{U}S$ with a modified matrix $\mathbf{A}S$, which is often called the capacitance matrix. The matrices $\mathbf{B}T_p$ and $\mathbf{C}T_p$ are sparse and it is possible to avoid fill-in. Then $\mathbf{U}S$ is back-substituted in the equation for the $\mathbf{U}V_p$ and the $\mathbf{U}V_p$ are calculated. This procedure may fail if the $\mathbf{A}T_p$ and the modified matrix $\mathbf{A}S$ are ill-conditioned. As a precaution, all condition numbers are estimated by the algorithm given in Reference 8.

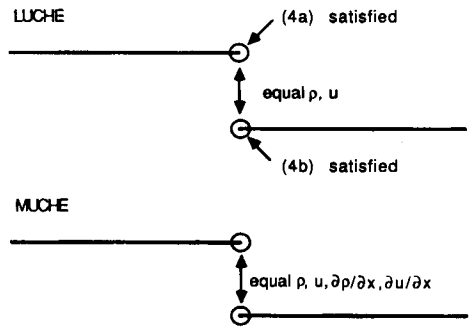

Figure 3(a). Conditions pertinent to interfaces with one point in common

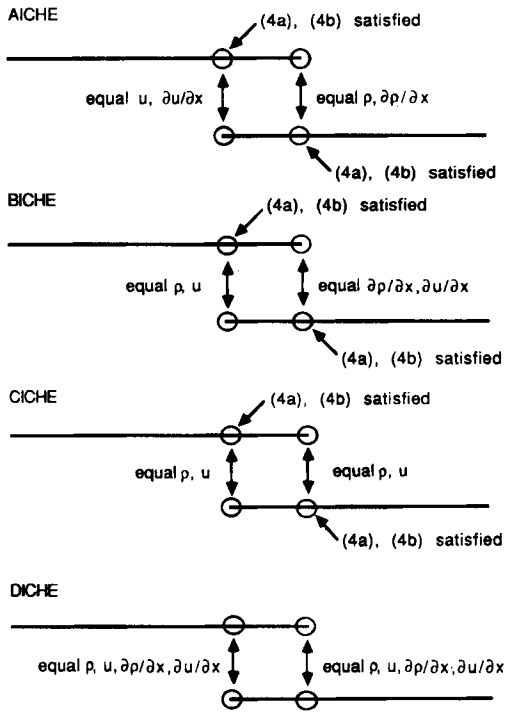

Figure 3(b). Conditions pertinent to interfaces with two points in common

RESULTS

Short-time results and accuracy

The errors appearing when solving (1) are classified as follows.

(1)→(2), time discretization error
(2)→(3), linearization error
(3)→(5), space discretization error
(5) is solved, round-off error.

Table I. Average increment AI after 20 time steps. Initial solution CFS. Code MUCHE. $N = 32$, $Q = 1$

AI	$0{\cdot}3 \times 10^{-14}$	$0{\cdot}3 \times 10^{-5}$	$0{\cdot}3 \times 10^{0}$	$0{\cdot}2 \times 10^{1}$	$0{\cdot}2 \times 10^{2}$	$0{\cdot}3 \times 10^{0}$	$0{\cdot}3 \times 10^{-5}$	$0{\cdot}2 \times 10^{-13}$
CF	6400	6400	6400	400	20	20	20	20
NI	3	2	1	1	1	2	3	4

These errors are functions of the time step Δt and of the parameters N and Q which determine the spatial resolution.

Of course a small Δt gives a small time discretization error by the Crank–Nicolson scheme. But a small Δt also yields a small round-off error. In fact the matrices connected with the solution of the boundary value problem (5) become better-conditioned as Δt shrinks and the round-off error consequently decreases. This effect, however, is difficult to evaluate quantitatively since the condition numbers also depend on the shape of ρ and u, the spatial resolution and the patching (see Table II). The symbols ρ and u have here resumed their original senses. Hence ρ and u stand for density and velocity respectively.

In addition, as Δt shrinks, the changes of ρ and u between adjacent time levels diminish. Therefore the average increment from one Newton iteration to another is a decreasing function of the computational frequency CF ($=2/\Delta t$). Table I confirms this fact. Here the average increment AI is one-fifth of the sum of the moduli of the increments of ρ, u, $\partial\rho/\partial x$, $\partial u/\partial x$ and $\partial^2 u/\partial x^2$ at the nodes, divided by the number of nodes. The number of Newton iterations is designated NI. Obviously, the increments decrease rapidly as the number of Newton iterations increases; the functions ρ_k u_k converge rapidly towards ρ^n, u^n. Analogous results apply for $Q > 1$.

The multidomain technique permits a good spatial resolution of the physical interval $[-1, 1]$ without increasing the order of the matrix equations which have to be solved by LU decomposition. Indeed, the number of nodes in each subinterval, $N + 1$, is chosen so large that one can benefit from exponential convergence, and so small that the round-off errors are not serious. The number of subintervals, Q, is then adjusted so that the functions ρ and u are smooth enough in each subinterval. The parameters CF = 20, $N = 12$, $Q = 5$ or CF = 20, $N = 16$, $Q = 3$ give a balanced result where the errors due to space integration are of the same order of magnitude as those due to time integration. In general, two Newton iterations are demanded for CF = 20. Using these parameter values, all tested procedures give accurate solutions after one time step, at $t = 0{\cdot}1$. However, as shown below, only AICHE, CICHE and MUCHE are long-time stable. By comparing the outcomes of different runs, it is found that four significant figures ρ and u result for $t \in [0, 10]$ using any long-time-stable code. If better accuracy is desired, one can choose CF = 800. Now it turns out that only one Newton iteration is sufficient.

These results are obtained using double precision on a 32 bit computer with intrinsic programmes such that

$$\cos(\tan^{-1} 1) = 0{\cdot}57 \times 10^{-17}.$$

Long-time results and stability

The stability properties depend mainly on the initial values ρ and u, the parameters CF, N and Q, as well as on the patching. Table II gives the time when numerical disturbances develop. Of course the errors evolve gradually and the given times are approximate.

The condition number of the modified matrix AS, COND, has been shown since the unknowns at the interfaces are calculated first by the procedure used to solve (5). Hence the round-off errors connected with this calculation are transferred also to the other unknowns. However, there does not seem to be any simple relation between the round-off errors and the stability. In Table II the

Table II. Time TI when instability appears. CF = 20, NI = 1

	Constant-flux initial solution		Equilibrium initial solution	
Code	TI	COND	TI	COND
AICHE $N = 12, Q = 5$	>10	$0{\cdot}4 \times 10^4$	>10	$0{\cdot}4 \times 10^4$
BICHE $N = 12, Q = 5$	0·2	$0{\cdot}6 \times 10^3$	2	$0{\cdot}1 \times 10^5$
CICHE $N = 12, Q = 5$	>10	$0{\cdot}5 \times 10^3$	>10	$0{\cdot}7 \times 10^3$
DICHE $N = 12, Q = 5$	7	$0{\cdot}1 \times 10^5$	>10	$0{\cdot}9 \times 10^4$
MUCHE $N = 12, Q = 5$	>10	$0{\cdot}3 \times 10^3$	>10	$0{\cdot}4 \times 10^3$
MUCHE $N = 32, Q = 1$	4		>10	
MUCHE $N = 2, Q = 30$	2	$0{\cdot}2 \times 10^3$	>10	$0{\cdot}2 \times 10^3$
LUCHE $N = 12, Q = 5$	0·6	$0{\cdot}3 \times 10^7$	0·8	$0{\cdot}8 \times 10^5$

computational frequency CF equals 20. Increasing CF leads to a more stable procedure. Detailed studies have been performed for MUCHE with $Q = 1$ in Reference 5. The number of Newton iterations has little influence on the stability properties.

Among the procedures above, AICHE, CICHE and MUCHE with $N = 12, Q = 5$ are the most stable ones. The procedures AICHE and BICHE are similar, but BICHE is unstable. In BICHE the function ρ and its derivative $\partial\rho/\partial x$ are not patched at the same point in the overlap, whereas they are in AICHE. The same is true for u and $\partial u/\partial x$ (see Figure 3(b)). As observed by the reviewer, in BICHE the requirements on ρ, u and $\partial\rho/\partial x$, $\partial u/\partial x$ are too weak for ensuring unique ρ and u, and an instability develops.

The scheme LUCHE is also unstable. Looking at the outcomes from runs with LUCHE, one observes that the first sign of instability is the behaviour of the derivatives $\partial\rho/\partial x$ and $\partial u/\partial x$. They vary slowly in the bulk of each subinterval and rapidly at the end points after a small number of time steps. The coupling between the subintervals seems to be insufficient. Alternatively, consider an interior subinterval of LUCHE. Equation (4a) is collocated at the right end and (4b) at the left end; compare Figure 3(a). It is now of interest to alter CICHE in such a way that (4a) be collocated twice at the two right end points and (4b) twice at the left ones. This form of CICHE is similar to LUCHE and they both have bad stability properties. Hence the instability of LUCHE may be attributed to a rather unsymmetric collocation of the governing equations.

The weakly unstable procedure DICHE is similar to MUCHE which is stable. However, the number of nodes where (4a, b) are not collocated is larger in DICHE than in MUCHE. In addition, the round-off error is larger in DICHE than in MUCHE.

Two extreme cases of MUCHE are also considered. The one-domain version ($N = 32, Q = 1$) is not as good as the multidomain approximation with spectral accuracy in each subdomain ($N = 12, Q = 5$). Also, the version with $N = 2, Q = 30$ is unsatisfactory. This degenerate spectral method is a second-order spline function approximation of ρ and u with low accuracy.

Table III. Error development. Equilibrium initial solution (AES). Code MUCHE. CF = 20, NI = 1

		$N = 12, Q = 5$	$N = 32, Q = 1$
$t = 1$	$\lvert\rho - \rho_{eq}\rvert$ at $x \approx -1$	$0{\cdot}8 \times 10^{-12}$	$0{\cdot}3 \times 10^{-10}$
	$\lvert\rho - \rho_{eq}\rvert$ at $x \approx 1$	$0{\cdot}5 \times 10^{-7}$	$0{\cdot}7 \times 10^{-7}$
	$\max\lvert\rho - \rho_{eq}\rvert$	$0{\cdot}5 \times 10^{-7}$	$0{\cdot}7 \times 10^{-7}$
	$\lvert\int_{-1}^{1}(\rho - \rho_{eq})dx\rvert$	$0{\cdot}7 \times 10^{-8}$	$0{\cdot}8 \times 10^{-8}$
	AI	$0{\cdot}5 \times 10^{-8}$	$0{\cdot}3 \times 10^{-5}$
$t = 10$	$\lvert\rho - \rho_{eq}\rvert$ at $x \approx -1$	$0{\cdot}5 \times 10^{-9}$	$0{\cdot}2 \times 10^{-8}$
	$\lvert\rho - \rho_{eq}\rvert$ at $x \approx 1$	$0{\cdot}4 \times 10^{-7}$	$0{\cdot}5 \times 10^{-7}$
	$\max\lvert\rho - \rho_{eq}\rvert$	$0{\cdot}2 \times 10^{-6}$	$0{\cdot}3 \times 10^{-6}$
	$\lvert\int_{-1}^{1}(\rho - \rho_{eq})dx\rvert$	$0{\cdot}1 \times 10^{-6}$	$0{\cdot}2 \times 10^{-6}$
	AI	$0{\cdot}1 \times 10^{-8}$	$0{\cdot}7 \times 10^{-6}$

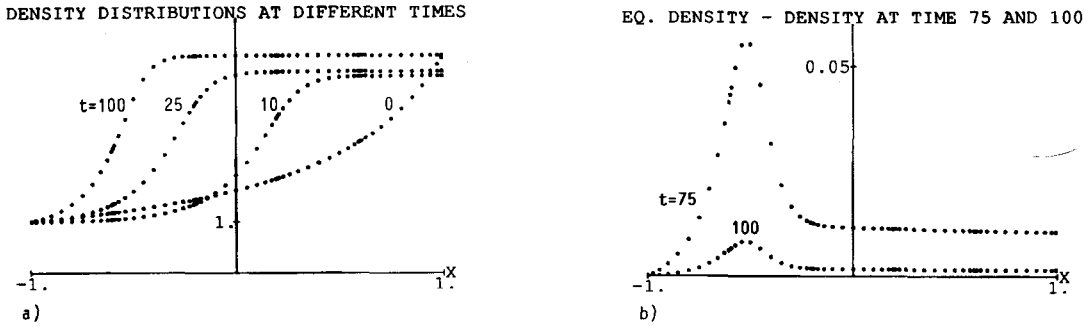

Figure 4. (a) Time history of the density profile. Initial solution CFS. Code MUCHE. CF = 20, NI = 2, $N = 12$, $Q = 5$. (b) Equilibrium value of ρ minus value of ρ at $t = 75$ and $t = 100$. The same run as in (a)

The error development is studied in detail using MUCHE with the equilibrium solution as the initial and the reference one. After a short time the errors of ρ and u are largest at the outflow. Then the errors spread upstream and reach a maximum near the inflow; the maximum is at $x \approx -0{\cdot}6$ for $t = 10$. No unphysical ripples appear and the average increment AI decreases monotonically as time increases. It seems as if the density and velocity distributions approach new, slightly altered equilibrium solutions. As a rule the errors of u and $\partial u/\partial x$ are less than the errors of ρ and $\partial\rho/\partial x$ respectively at corresponding points. Some numerical data are given in Table III.

Another interesting test of the code MUCHE has been performed. Using MUCHE, one can follow how the constant-flux initial solution (CFS) evolves towards equilibrium. As illustrated in Figure 4, at $t = 100$ the density differs by less than 0·01 from its equilibrium value and the difference has a maximum where the profile is steep. No disturbances are visible.

The codes AICHE and CICHE with CF = 20, NI = 2, $N = 12$, $Q = 5$ have passed the same long-time test. At time $t = 100$ MUCHE, AICHE and CICHE yield ρ and u where corresponding values agree to within four or five significant figures.

CPU time

Using the code MUCHE, the number of operations required to reach the solution at time t is of the order of magnitude

$$t \cdot \mathrm{CF} \cdot \mathrm{NI} \cdot \{Q[2(N-1)]^3 + (4Q)^3\}$$

In fact the CPU time is almost the same for $N=12$, $Q=5$ as for $N=16$, $Q=3$, while $N=32$, $Q=1$ takes roughly three times longer machine time. On a Macintosh II the CPU time is 6·5 min for a run with $t \cdot \mathrm{CF} \cdot \mathrm{NI} = 100$ and $N = 12$, $Q = 5$ or $N = 16$, $Q = 3$.

As a rule the codes AICHE and CICHE demand more CPU time than MUCHE for comparable runs. The run mentioned above with $N = 12$, $Q = 5$ takes 7·5 min for AICHE or CICHE.

ACKNOWLEDGEMENTS

The reviewer has suggested the patching conditions corresponding to the procedures AICHE, CICHE and LUCHE. The author thanks Dr. Staffan Bergwall for his critical reading of the manuscript.

REFERENCES

1. C. Basdevant, M. Devile, P. Haldenwang, J. M. Lacroix, J. Onazzani, R. Peyret, P. Orlandi and A. T. Patera, 'Solutions of the Burger equation', *Comput. Fluids*, **14**, 23–41 (1986).
2. G. Macaraeg and C. L. Street, 'Improvements in spectral collocation discretization through a multiple domain technique', *Appl. Numer. Math.*, **2**, 95–108 (1986).
3. G. B. Whitham, *Linear and Nonlinear Waves*, Wiley, New York, 1974, p. 190.
4. D. E. Gray (ed.), *American Institute of Physics Handbook*, McGraw-Hill, New York, 1972, p. 2/235.
5. B. Kjellmert, 'Chebyshev pseudospectral solution of a one-dimensional flow problem', *Report Tulea 1988:17*, Luleå University of Technology, 1988.
6. H. L. Ku and D. Hatziavramidis, 'Chebyshev expansion methods for the solution of the extended Graetz problem', *J. Comput. Phys.*, **56**, 495–512 (1984).
7. D. E. Keyes and W. D. Gropp, 'A comparison of domain decomposition techniques for elliptic partial differential equations and their parallel implementation', *SIAM J. Sci. Stat. Comput.*, **8**, 166–202 (1987).
8. G. E. Forsythe, M. A. Malcolm and C. B. Moler, *Computer Methods for Mathematical Computations*, Prentice-Hall, Englewood Cliffs, NJ, 1977, p. 48.